Superlattices and Microstructures 118 (2018) 170–176

Contents lists available at ScienceDirect

Superlattices and Microstructures

journal homepage: www.elsevier.com/locate/superlattices

Thermal annealing induced the tunable optical properties of silver thin films with linear variable thickness

Ruijin Hong [a, b], Wen Shao [a], Jialin Ji [a], Chunxian Tao [a], Dawei Zhang [a, *]

[a] Engineering Research Center of Optical Instrument and System, Ministry of Education and Shanghai Key Lab of Modern Optical System, University of Shanghai for Science and Technology, No. 516 Jungong Road, Shanghai, 200093, People's Republic of China
[b] State Key Laboratory of Applied Optics, Changchun Institute of Optics, Fine Mechanics and Physics, Chinese Academy of Sciences, Changchun, 130033, People's Republic of China

ARTICLE INFO

Article history:
Available online 5 April 2018

Keywords:
Silver thin film
Surface plasmons
Surface enhanced raman scattering
Absorption spectra

ABSTRACT

Silver thin films with linear variable thickness were deposited at room temperature. The corresponding tunability of optical properties and Raman scattering intensity were realized by thermal annealing process. With the thickness increasing, the topography of as-annealed silver thin films was observed to develop from discontinued nanospheres into continuous structure with a redshift of the surface plasmon resonance wavelength in visible region. Both the various nanosphere sizes and states of aggregation of as-annealed silver thin films contributed to significantly increasing the sensitivity of surface enhanced Raman scattering (SERS).

1. Introduction

Surface plasmons (SPs) are collective electronic excitations at the interface between metals and dielectrics, and are currently being explored for their potential applications in subwavelength optics [1,2], data storage [3,4], nonlinear optics [5–7], surface enhanced Raman scattering (SERS) [8–12], catalysis, and biophotonics [13–16]. Especially, metallic nanostructures with tunable localized surface plasmonic resonance (LSPR) have potential applications in surface enhanced Raman scattering and biosensing [17,18]. Tunable LSPR is reported in different matrices [8–11] using configurations of multilayers [10] and core-shell nanoparticles [8,19]. Therefore, of great significance is the ability to tune and extend the plasmon resonance wavelength, which is highly desirable in various applications of metallic nanoparticles [20,21].

The vast majority of investigations of LSPRs have been focused on noble metals, being stable under a wide range of conditions and having a high charge carrier density [22–24]. Noble metal, in particular silver nanostructures with strong and tunable surface plasmon resonance (SPR) from visible to near-infrared spectral regions, has efforts to fabricate nanostructure-based SERS substrates [25,26]. Silver has been of considerable interest for years due to their better performance relative to other metal in optical properties [27]. The plasmon resonance energy of metal nanoparticles (NPs) depends on the metal shape and size, crystallization, structure and the nature of the environment of the assembled particles [28,29]. Several methods have been used for the fabrication of nanoparticles. However, difficulty in obtaining monodisperse nanoparticles sizes and their tendency to aggregate hinders these exciting properties for applications challenging.

* Corresponding author.
E-mail address: dwzhang@usst.edu.cn (D. Zhang).

https://doi.org/10.1016/j.spmi.2018.04.008
0749-6036/

In this paper, we propose an alternative cost-effective technique that enables nanofabrication of silver nanospheres by using a very simple fabrication procedure. The technique includes only standard fabrication steps, such as silver thin film deposition with linear variable thickness and thermal annealing process. The influences of linear variable thickness on the topography, structure, optical absorption and Raman scattering properties of silver nanospheres were discussed in the paper. The finite difference time domain (FDTD) method was employed to calculate electronic-field distribution of silver nanospheres with various sizes and states of aggregation.

1.1. Experimental and characterizations

Silver thin film with linear variable thickness was deposited on a silica substrate by magnetron sputtering using a silver target (99.99%) at room temperature. The deposition chamber was evacuated to a base pressure of about 5×10^{-4} Pa and the working pressure was 0.8 Pa. The substrate size is 100 mm in length, 50 mm in width, and 1.4 mm in thickness, respectively. Prior to deposition, the thickness was calibrated to ensure its accuracy, and the thickness of as-deposited silver layer varied from 5 nm to 30 nm, which was monitored by a situ quartz crystal microbalance. The as-deposited sample was placed in a thermal treatment furnace under ambient condition with the process as following: the as-deposited silver thin film were put into an as-heated furnace of 300 °C and maintained for 10 min. We divided the sample into five zones along the length direction, and named the zone from the thinner side to the thicker side before and after thermal annealing as sample 1(S1) (sample 1′(S1′)), sample 2(S2) (sample 2′(S2′)), sample 3(S3) (sample 3′(S3′)), sample 4(S4) (sample 4′(S4′)), and sample 5(S5) (sample 5′(S5′)), respectively. The schematic structure of the sample is shown in Fig. 1.

The crystal structure of the film was characterized by x-ray diffraction (XRD) using a Bruker AXS/D8 Advance system, with Cu Kα radiation ($\lambda = 0.15408$ nm). The optical absorption of the samples was measured with an UV-VIS-NIR double beam spectrophotometer (Lambda 1050, Perkins Elmer). The surface roughness was examined by Atomic force microscopy (AFM) (XE-100, Park Systems) with scanning area for 3 μm × 3 μm. The scanning electron microscopy (SEM) images were taken on the Hitachi S-4800. Raman Scattering spectra were acquired using a confocal microprobe Raman system (LabRam Aramis, Horiba) operated with a DPSS blue laser (473 nm). The size of laser spot is about 1 μm in diameter. The SERS substrates were prepared according to the following procedure: firstly, 20 mL Rh B solution with the concentration of 10^{-7} mol/L (M) in ethanol was prepared. Then, Rh B solution was dosed onto silver thin film surface with five drops for each sample using a dropper. Then, the solution was dried under a N_2 flow. Finally, the as-dosed substrates were ready for SERS measurement. All the measurements were carried out at room temperature.

2. Results and discussion

Fig. 2 shows the SEM images of the plan-view silver thin film before and after thermal annealing, respectively. According to Fig. 2(a), the as-deposited silver thin film shows a wetter morphology with the substrate, no obvious particles were observed on it. However, the annealing process is found to have a profound effect on the morphology of silver thin films. The as-annealed silver thin films exhibits dewetting, consisting of silver nanosphere particles with different sizes and different aggregation states. Obviously, the silver nanospheres are distributed homogeneously on the substrates with sizes ranging from 30 nm to 150 nm. With the thickness increasing, the size silver nanosphere increased while the state of aggregation decreased. In general, the surface oxide seems to block surface and/or grain boundary diffusion paths, and prevents the dewetting of the film from the substrate until the melting point. However, for the rapid thermal annealing process, the temperature was elevated in a short time. The high temperature, instability driven, breaks up the film into droplets with nanosize solid metallic particles, causing the film to de-wet the substrate.

XRD patterns as shown in Fig. 3 reveal the influence of thickness and thermal annealing process on the structure of silver thin film. According to Fig. 3(a), with the increase of film thickness, a strongest diffraction peak appears at around 38.60° (2θ) in as-deposited films corresponding to the (111) crystallographic plane. Additionally, the phase of silver thin film varied from amorphous to polycrystalline with a face centered cubic (fcc) crystal structure, which is corresponding to standard card of silver (JCPDS: 04–0783). It indicates a preferential orientation of the silver grains along the (111) crystallographic direction. In general, for the non-epitaxial deposition on a substrate, the surface of film tends to be either a (111) or (0001) plane due to the

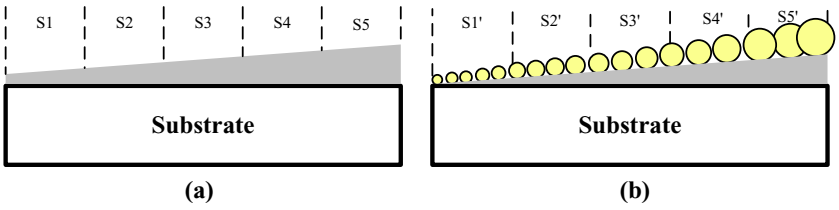

Fig. 1. Schematic structures of samples (a) before and (b) after thermal annealing.

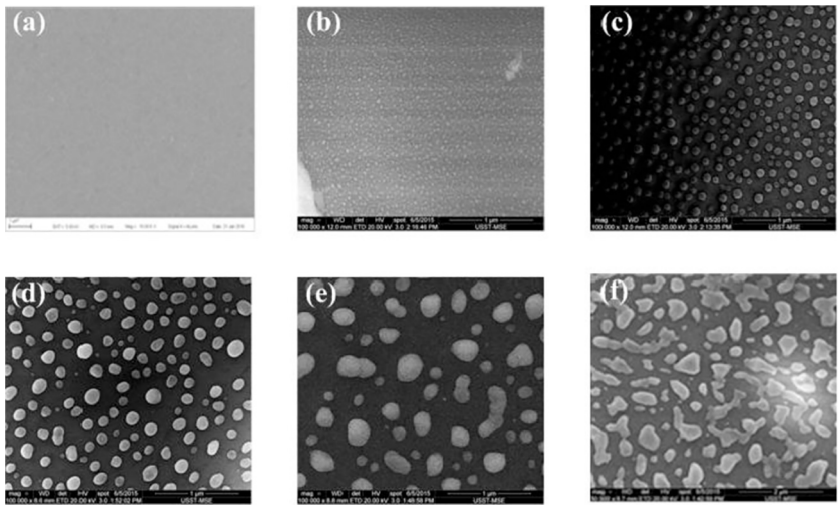

Fig. 2. SEM images of (a) as-deposited and (b–f) as-annealed silver thin films with various thicknesses.

minimum surface free energy in these planes, meaning that the (111) textured film must form in an effective equilibrium state where enough surface mobility is given to impinging atoms under a certain deposition condition. As shown in Fig. 3(b), the as-annealed films have higher intensity, sharper peaks and show stronger (111) orientations compared to the corresponding as-deposited films with the increase of thickness. According to the standard card of silver (JCPDS: 04–0783), the inter-planar spacing of silver powder (111) plane is 0.2359 nm, while for the silver thin films, the inter-planar spacing of (111) plane is about 0.2330 nm. The discrepancy in d-value is due to the residual stress developed in the films.

Optical absorption is very important in characterizing the active substrate for surface-enhanced spectroscopy because it reflects the surface plasma resonance in the films. The optical absorption spectra obtained from silver thin films before and after annealing are shown in Fig. 4. According to Fig. 4(a), an absorption peak at about 320 nm with a broad shoulder at the low energy side, corresponding to the plasma edge of silver, is observed in the as-deposited silver thin film with 5 nm. Along with the increase of silver layer thickness, the absorption peak becomes sharper and the shoulder decreases. Also, no obvious LSPR absorption peaks are observed in the as-deposited samples. For the as-deposited silver thin films, when light is incident on the smooth silver thin film surface, the light waves are trapped on the surface due to their interaction with the free electrons of the metal. At the same time, these waves are converted into an surface plasmons mode which propagates along the interface and gradually attenuates for the internal absorption from silver thin film [30]. However, a noticeable broadband corresponding to LSPR absorption peak appears in the range of 460–480 nm from the as-annealed samples (as shown in Fig. 4(b)). The absorption peak intensity increases and the peak positions show a red shift with silver thickness increasing since the globular particles were formed in the case of thermal annealing process. The incident light, being absorbed by the globular silver particles, can cause the localized electromagnetic field coupling between them, which plays an important role in tuning the LSPR peak position and intensity. These results show that plasmonic coupling takes place when the silver globular particles are close to each other and the plasmon resonance of each particle is affected by plasmon resonance of its neighboring particles. The increased distance between the silver particles due to the increasing thickness results in collective coupled oscillations of surface plasmon at longer wavelengths. On the other hand, the strength of plasmonic coupling depends on the sizes of particles, the distance between particles and the state of aggregation.

Fig. 5 shows the representative AFM micrographs with a scanning area of 3 $\mu m \times 3\ \mu m$ obtained from silver thin films before and after annealing, respectively. The surface roughness values (Rq) of as-deposited samples range from 1.715 to 3.126 nm increased with the thickness increasing (as shown in Fig. 6). For the thinner side of the sample, the value of surface roughness is low due to the smooth substrate. With the film thickness increasing, the microstructural evolution varies from amorphous to polycrystalline phase, inducing grain coarsening or shadowing effects and resulting in the increasing of surface roughness of thin films. To reduce surface energy, silver atoms begin to aggregate in the film to form silver nanospheres in the case of annealing. It is easy to obtain the various sizes of silver nanospheres by thermal annealing the silver thin film with linear variable thickness. The surface roughness values of as-annealed samples range from 3.827 nm to 29.425 nm increased with the thickness increasing. The SEM plan-view images of the as-annealed films could be also given as evidence for the variation of surface roughness.

To study the potential application of the proposed silver thin films, these samples before and after annealing were used as the SERS substrates. Probing Rhodamine B (Rh B) molecules is a typical artificial dye and was chosen as a test compound (concentration = 0.1 μM) for researching the application of silver thin film with linear variable thickness to detect trace toxic

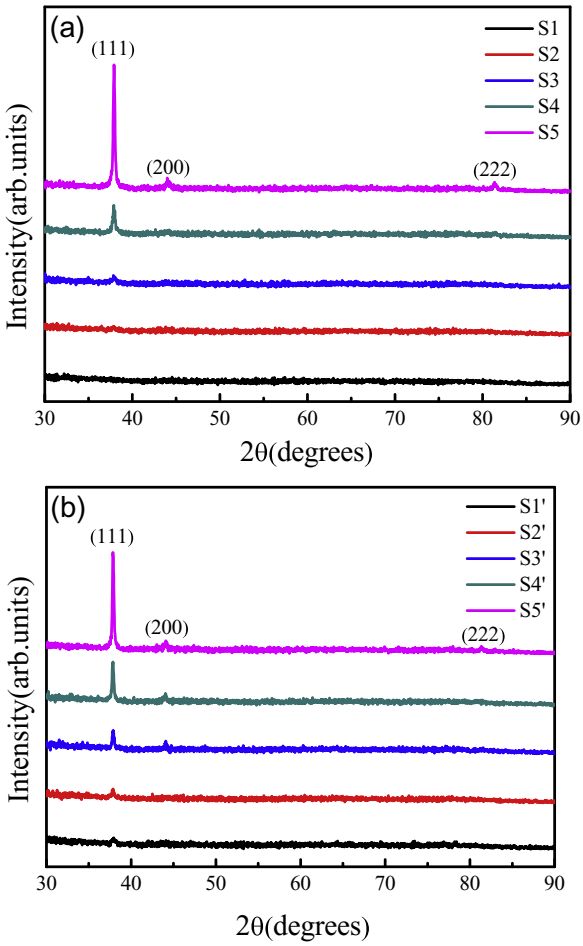

Fig. 3. XRD patterns of (a) as-deposited and (b) as-annealed silver thin films.

organic compounds. In this experiment, the Rh B molecule solutions were dosed onto the silver thin films surface. Fig. 7 shows the detected SERS spectra of the Rh B molecules on the as-deposited and as-annealed silver thin films. Three strong Raman bands at about 1648, 1361 and 1504 cm^{-1}, being assigned to the C=C stretching mode of aromatic rings [31], were clearly observed in all samples. For the as-deposited samples (Fig. 7(a)), the SERS signal intensity collected from the thinner silver thin film was very weak, while the signal intensities were enhanced significantly with the thickness increasing. The SERS enhancement can be solely attributed to the roughness. These SERS experimental results are consistent with the AFM results. For the as-annealed samples shown in Fig. 7(b), the SERS signal intensity enhanced with the thickness increasing and then decreased in S5'. The SERS enhancement can be attributed to the roughness, the silver particles sizes and aggregation states. However, when the increased size and the decreased aggregation states of Ag particles reach a certain degree, there are less "hot spots" to excite the local electrical fields, resulting in the decrease of Raman intensity. These SERS experiments provide concrete evidence that the as-annealed silver thin film has much better SERS performance than the as-deposited silver thin film, owing to the much stronger field localization and significant enhancement in the silver particles. Therefore, the silver thin film has great potential to be used as a low-cost, replicable, high-performance active substrate for SERS applications.

To further verify these points above, The FDTD method, a well-known theoretical simulation one, was employed to calculate the electric field distribution of the silver thin films surface with different particles sizes and aggregation states. Fig. 8 shows the calculated electric field intensity spatial distributions in as-deposited and as-annealed silver thin films. In this calculation, a 470 nm laser irradiates perpendicularly to the x-y plane of the silver system with the polarization along the y axis direction. In Fig. 8(a), we can see that the electric field intensity increases linearly with increasing silver thin film thickness. The simulation results revealed that the surface roughness contributed to the major enhancement of the electric field. Fig. 8(b)–(f) exhibit the calculated electric field intensity spatial distributions in as-annealed silver thin films with different particles sizes and different aggregation states, respectively. The "hot spots" are obviously formed on the surfaces,

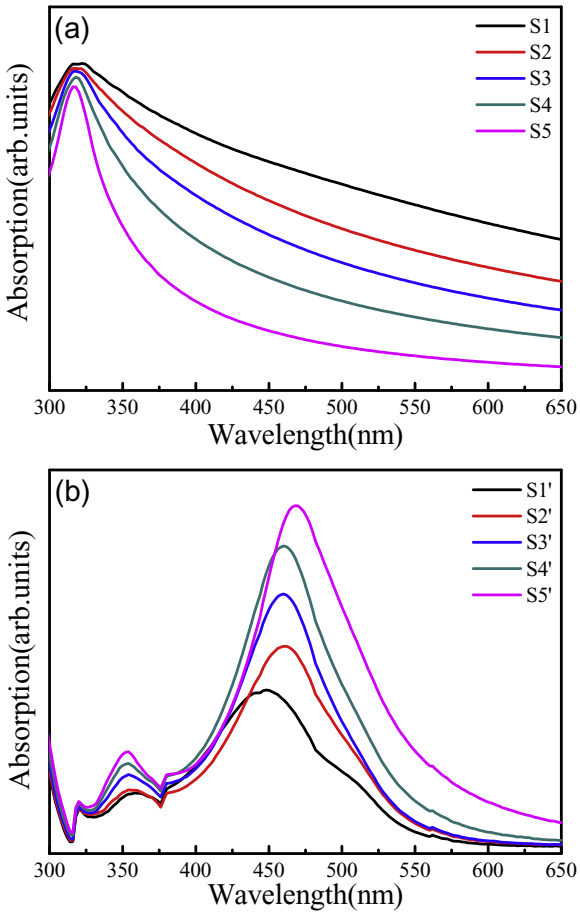

Fig. 4. Optical absorption spectra of (a) as-deposited and (b) as-annealed silver thin films.

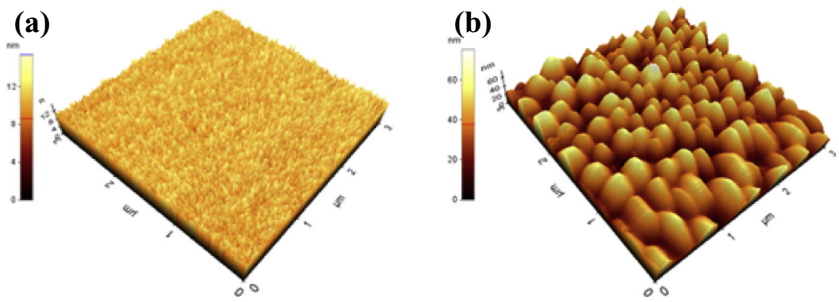

Fig. 5. AFM images for silver thin films (a) before and (b) after thermal annealing.

and the intensity of the electric field increases with the thickness increasing up to 30 nm and then abruptly decreased with further increasing of thickness. The FDTD simulation results revealed that the particles sizes and aggregation states contributed to the major enhancement of the electric field because of the present of the high-density “hot spots,” and this enhancement is actually due to the EM resonant excitation of LSPRs. Those calculation results are in good agreement with those of experiments above.

3. Conclusions

In conclusion, the tunable optical properties of silver thin films with linear variable thickness were realized by thermal annealing process. The LSPR wavelength depends on the thickness of silver thin films. With increased silver layer thickness,

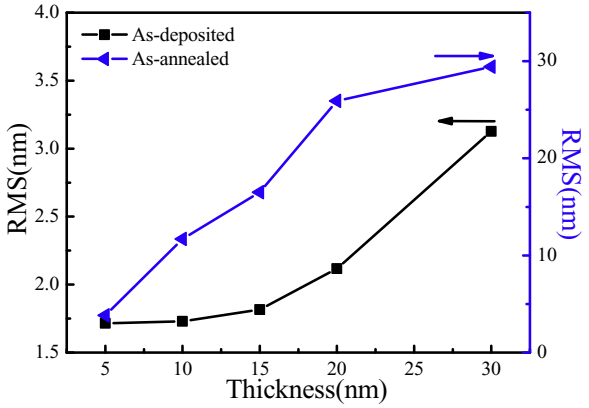

Fig. 6. Variations of surface roughness for silver thin films before and after thermal annealing.

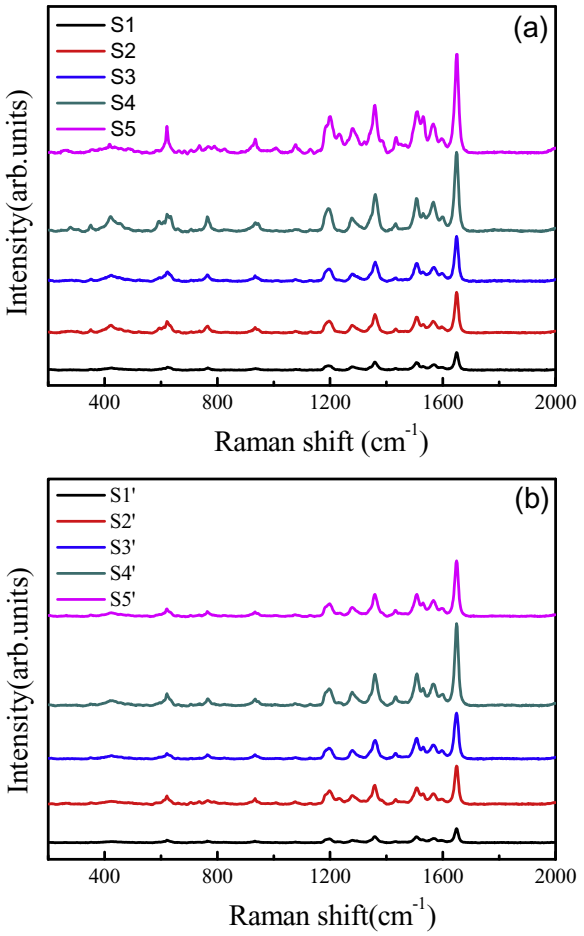

Fig. 7. Raman scattering spectra of Rh B on (a) as-deposited and (b) as-annealed silver thin films.

the resonance wavelength has a red shift which is attributed to the surface roughness, nanosphere sizes and states of aggregation of silver thin film. Additionally, the FDTD calculation result shows good agreement qualitatively with the Raman experimental data. This is an experimental demonstration of LSPR tuning in the silver thin films with linear variable thickness in summary.

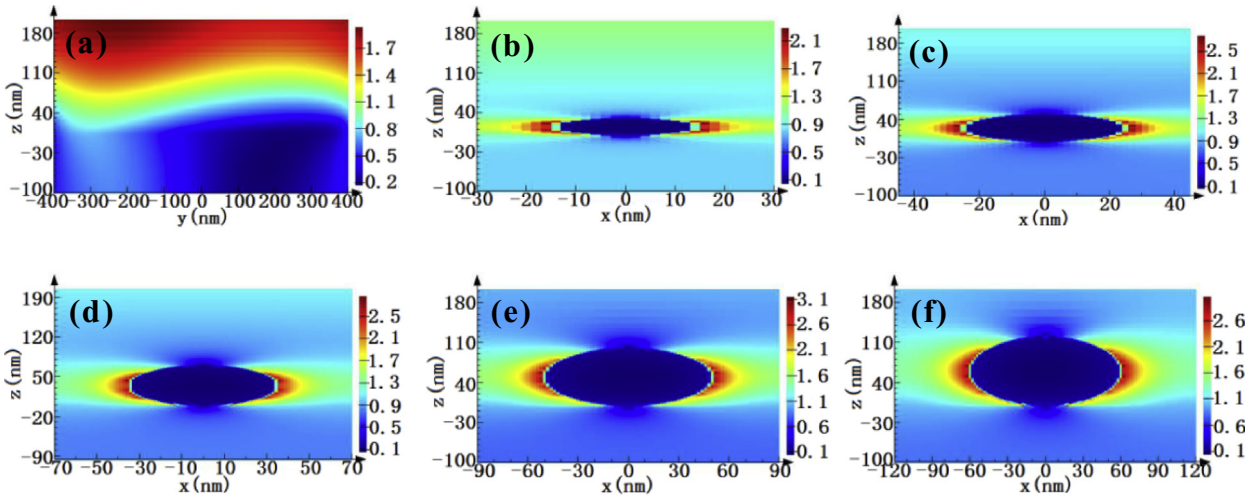

Fig. 8. FDTD simulated electric field amplitude patterns for (a) as-deposited and (b–f) as-annealed silver thin film.

Acknowledgments

This work was partially supported by the National Natural Science Foundation of China (61775140, 61775141) and the National Key Research and Development Program of China (2016YFB1102303).

References

[1] J. Dintinger, S. Klein, F. Bustos, W.L. Barnes, T.W. Ebbesen, Phys. Rev. B 71 (2005) 035424.
[2] E. Aznar, M.D. Ma, R. Martínez-Máñez, F. Sancenón, J. Soto, P. Amorós, C. Guillem, J. Am. Chem. Soc. 131 (2009) 6833.
[3] L.A. Peyser, A.E. Vinson, A.P. Bartko, R.M. Dickson, Science 291 (2001) 103.
[4] J. Qiu, X. Jiang, C. Zhu, M. Shirai, J. Si, N. Jiang, Angew. Chem. Int. Ed. 43 (2004) 2230.
[5] Y. Yang, M. Nogami, J. Shi, H. Chen, G. Ma, S. Tang, Appl. Phys. Lett. 88 (2006) 081110.
[6] Y. Yang, M. Nogami, J. Shi, H. Chen, Y. Liu, S. Qian, J. Mater. Chem. 13 (2003) 3026.
[7] Y. Yang, M. Nogami, J. Shi, H. Chen, G. Ma, S. Tang, J. Phys. Chem. B 109 (2005) 4865.
[8] S. Nie, S.R. Emory, Science 275 (1997) 1102.
[9] C.L. Haynes, A.D. McFarland, R.P. Van Duyne, Anal. Chem. 77 (2005) 338A.
[10] S.B. Chaney, S. Shanmukh, R.A. Dluhy, Y.P. Zhao, Appl. Phys. Lett. 87 (2005) 031908.
[11] I.S. Lim, J. Ouyang, J. Luo, L. Wang, S. Zhou, C. Zhong, Chem. Mater. 17 (2005) 6528.
[12] Y. Yang, L. Xiong, J. Shi, M. Nogami, Nanotechnology 17 (2006) 2670.
[13] C.J. Murphy, N.R. Jana, Adv. Mater. 14 (2002) 80.
[14] T.A. Taton, C.A. Mirkin, R.L. Letsinger, Science 289 (2002) 1757.
[15] Y. Lou, M.M. Maye, L. Han, J. Luo, C.J. Zhong, Chem. Commun. 5 (2001) 473.
[16] M.M. Maye, J. Luo, L. Han, C.J. Zhong, Nano Lett. 1 (2001) 575.
[17] A.J. Haes, R.P. Van Duyne, Anal. Bioanal. Chem. 379 (2004) 920.
[18] B. Pettinger, K.F. Domke, D. Zhang, R. Schuster, G. Ertl, Phys. Rev. B 76 (2007) 236401.
[19] Y.B. Zheng, T.J. Huang, A.Y. Desai, S.J. Wang, L.K. Tan, H. Gao, Appl. Phys. Lett. 90 (2007) 183117.
[20] S. Link, M.A. El-Sayed, J. Phys. Chem. B 103 (1999) 4212.
[21] A. Biswas, O.C. Aktas, U. Schurmann, U. Saeed, V. Zaporojtchenko, F. Faupel, Appl. Phys. Lett. 84 (2004) 2655.
[22] M. Barbic, J.J. Mock, D.R. Smith, S. Schultz, J. Appl. Phys. 91 (2002) 9341.
[23] J.P. Kottmann, O.J. Martin, D.R. Smith, S. Schultz, Phys. Rev. B 64 (2001) 235402.
[24] K.H. Su, Q.H. Wei, X. Zhang, J.J. Mock, D.R. Smith, S. Schultz, Nano. Lett. 3 (2003) 1087.
[25] M. Fan, A.G. Brolo, Phys. Chem. Chem. Phys. 11 (2009) 7381.
[26] W. Song, X. Han, L. Chen, Y. Yang, B. Tang, W. Ji, Y. Ozaki, J. Raman Spectrosc. 41 (2010) 907.
[27] M. Baia, L. Baia, S. Astilean, J. Popp, Appl. Phys. Lett. 88 (2006) 143121.
[28] K.L. Kelly, E. Coronado, L.Z. Lin, G.C. Schatz, Cheminform 34 (2003) 668.
[29] A.R. Tao, S. Habas, P. Yang, Small 4 (2008) 310.
[30] W.L. Barnes, A. Dereux, T.W. Ebbesen, Nature 424 (2003) 824.
[31] T. Vosgröne, A.J. Meixner, J. Lumin. 107 (2004) 13.